The Single-Pass Cerebral Extraction and Capillary Permeability-Surface Area Product of Several Putative Cerebral Blood Flow Imaging Agents

Richard J. Di Rocco, Deborah A. Silva, Bruce L. Kuczynski, Rama K. Narra, Kondareddiar Ramalingam, Silvia Jurisson, Adrian D. Nunn and William C. Eckelman

The Bristol-Myers Squibb Pharmaceutical Research Institute, New Brunswick, New Jersey

We have determined cerebral blood flow (CBF) and the single-pass cerebral extraction (E) of several putative agents for external imaging of CBF. Simultaneous measurements of blood flow and extraction were performed in 106 rats. For all agents, comparison of linear and exponential regressions of E on CBF indicates that this relationship can be described as linear over the range of flows studied. Analysis of covariance indicates that the extraction of ^{123}I-IMP, ^{67}Cu-PTSM and ^{99m}Tc-HMPAO is higher than that of ^{99m}Tc-Cl(DMG)$_3$2MP and ^{99m}Tc-ECD, particularly at flows above the normal range. Accordingly, for ^{123}I-IMP, ^{67}Cu-PTSM and ^{99m}Tc-HMPAO, the slope of the linear regression equation for the relationship between brain capillary permeability surface area product (PS) and CBF is higher than that for ^{99m}Tc-Cl(DMG)$_3$2MP and ^{99m}Tc-ECD. PS varies as a linear function of CBF over the range of flows studied. At a CBF level that corresponds to normal regional CBF for human cortex, 0.5 ml/g/min, all the agents have a single-pass extraction of approximately 70% or greater. While all the agents detected changes in CBF in the normal to ischemic range, at higher flows ^{123}I-IMP, ^{67}Cu-PTSM and ^{99m}Tc-HMPAO showed substantially greater fidelity to true CBF than ^{99m}Tc-Cl(DMG)$_3$2MP and ^{99m}Tc-ECD.

J Nucl Med 1993; 34:641–648

Iodoamines (*1–3*) and a series of copper complexes (*4,5*) have been investigated as agents for imaging regional cerebral blood flow (rCBF) and one compound, ^{123}I-iodoamphetamine (IMP), is approved in the United States and Europe for stroke detection. Unfortunately, the best iodine and copper radionuclides are cyclotron produced and, therefore, have limited availability. Owing to the ready availability of $^{99m}TcO_4^-$, its 6 hr half-life and the pure gamma emission at 140 keV, ^{99m}Tc-labeled agents are better suited for external imaging of rCBF by SPECT. Initial work showing a single-pass cerebral extraction of 80% but a low brain residence time for ^{99m}Tc-PnAO (*6*) led to the subsequent preparation of ^{99m}Tc-HMPAO, a mixture of the d and l enantiomers of hexamethylpropyleneamine oxime (*7*). Technetium-99m-HMPAO has a high single-pass cerebral extraction in rats and humans (*8*) and is retained by the brain long enough to acquire data using a single-headed rotating SPECT camera. More recently, a diester N_2S_2 complex, ^{99m}Tc-L,L,-ethyl cysteinate dimer (^{99m}Tc-ECD), has been shown to cross the blood-brain barrier (BBB) in several species with adequate retention in primates and humans (*9–11*). We have developed a new class of neutral compounds known as boronic acid adducts of technetium dioxime complexes (BATOs). Details of the chemistry have been described elsewhere (*12,13*). One of these complexes (chloro [bis-{2,3-butanedionedioxime (1-)-}{2,3- butanedionedioximato (2-)- N, N′, N″, N‴, N⁗, N′⁗} (2-methylpropyl borato (2-) technetium]) (^{99m}Tc-Cl(DMG)$_3$2MP) is characterized by rapid blood clearance and brain uptake, adequate brain clearance half-time, high grey-to-white-matter ratio and a distribution pattern in monkey brain autoradiograms that is virtually identical to the cytoarchitectonic pattern of CBF (*14*).

An agent for imaging organ blood flow should have a high single-pass extraction and be rapidly cleared from the blood (*15*). Several studies have examined the single-pass cerebral extraction of the CBF imaging agents described above (*1,5,8,10,16,17*). In those studies, single-pass cerebral extraction (E) was determined using intracarotid injection of test substances in indicator dilution or B/A procedures and CBF was determined some time after E. Alternatively, E was measured using intracarotid injection of test and reference substances in a procedure for determination of a brain uptake index, in

Received Jul. 16, 1992; revision accepted Nov. 17, 1992.

For correspondence or reprints contact: Richard J. Di Rocco, The Bristol-Myers Squibb Pharmaceutical Research Group, 1 Squibb Dr., P.O. Box 191, New Brunswick, NJ 08903-0191.

which CBF was not measured at all. Accordingly, previous comparisons of different imaging agents have been presented in terms of average extraction across a range of flows, or simply extraction without specifying flow. This is unsatisfactory because in the Renkin-Crone equation, E is an exponential function of CBF and capillary permeability-surface area product, PS, according to: $E = 1 - e^{-PS/CBF}$ (*18,19*). In addition, sequential determination of CBF and E may introduce an error in the relationship between these variables. This is particularly true when the test substance is injected into the carotid artery (*1,5,10*) because intracranial pressure, cerebrovascular volume and CBF have been shown to increase with increased intracarotid injection volume (*20, 21*). Intravascular streaming and variable delivery of injectate also have been observed following intracarotid infusion of ^{14}C-iodoantipyrine (*22*). We avoided these problems by using an indicator fractionation method that requires the intracardial administration of a mixture of radiolabeled microspheres and test substance for the simultaneous determination of E and CBF (*23*).

When E and CBF are both measured, linear regressions of E on CBF are sometimes used to describe the relationship between these variables (*8,24*), but analysis of covariance has not been used to facilitate comparison of different agents across a full range of flows. Analysis of covariance is based upon a linear model, but a rigorous approach to its application would seem to require a comparison of linear and Renkin-Crone exponential models to determine which provides the best fit to the data. Unfortunately, according to the Renkin-Crone equation, E is a function of two variables. One solution to this problem assumes that PS is constant with respect to flow (*24,25*). Substitution of measured values of CBF and E into the Renkin-Crone equation to derive values for PS has shown, however, that PS varies with respect to CBF (*8,23,26*). Alternatively, it is possible to derive an expression for PS as a function of CBF, thereby rendering E a function of CBF alone. This modified form of the Renkin-Crone equation can then be used as a nonlinear regression model (*23*). Using this treatment, we were able to compare linear and nonlinear regressions of E on CBF, thereby providing a statistical justification for using the linear model and analysis of covariance to compare the performance of different imaging agents over a full range of clinically significant blood flows. In the present studies, we used an indicator fractionation method for the simultaneous determination of E and CBF as well as analysis of covariance to provide a comprehensive comparison of the single-pass extractions of ^{99m}Tc-Cl(DMG)$_3$2MP, ^{99m}Tc-ECD, ^{99m}Tc-HMPAO, ^{67}Cu(II)-pyruvaldehyde bis(methylthiosemicarbazone) (PTSM) and ^{123}I-IMP. The extraction of $^{99m}TcO_4^-$ and ^{99m}Tc-DTPA, which do not cross the BBB, were examined as controls.

MATERIALS AND METHODS

Animal Preparation

Data from 106 male Sprague-Dawley rats (250–350 g) are reported. The rats were anesthetized with Nembutal (50 mg/kg) and PE-50 femoral arterial catheters were implanted. The rats were tracheotomized and positioned with their necks in a guillotine. After thoracotomy, they were connected to a Harvard respirator with positive and expiratory pressure. The pericardium was then cut to expose the heart. Core temperature was monitored and maintained between 36° and 39°C. A range of CBF was normally obtained by controlling respiratory frequency (35–75 min^{-1}), but in some cases the tidal volume (1.3–1.7 ml) was also varied. Arterial blood samples were obtained from the arterial catheter and analyzed using a blood gas analyzer (CIBA-Corning, Medfield, MA). Normal CBF values centering on 0.5 ml/g/min were achieved by setting arterial P_aCO_2 at approximately 40 ± 3 mmHg. Higher CBF levels were obtained by raising P_aCO_2 levels to approximately 60 ± 3 mmHg.

Experimental Protocol

Once the desired blood gas parameters were stabilized, a syringe pump set to withdraw blood at a rate of 1.15 ml/min was connected to the femoral arterial catheter. This served as the reference organ. With the pump on, the injection mixture (see below) was rapidly (<0.5 sec) injected into the left ventricle. Six seconds postinjection, the rat was decapitated and the syringe pump was stopped simultaneously by a switch triggered by the guillotine. The 6-sec decapitation time recommended by Irwin and Preskorn (*23*) is based on a previous characterization of cerebral hemodynamics following 20 μl and 50 μl ^{14}C-inulin intracarotid bolus injections lasting less than 1 sec (*20*). The brain, heart and kidneys were removed within 3–4 min of decapitation and weighed. Technetium-99m, ^{123}I, ^{67}Cu and ^{85}Sr activities in the organs and arterial blood were measured with an LKB 1282 Commpugamma gamma counter, which corrected for cross-over counts for each radionuclide.

Autoradiography and Image Analysis

To depict rCBF after a 6-sec single-pass, ^{99m}Tc-Cl(DMG)$_3$2MP (9–12 mCi) was injected into each of three rats prepared as above and decapitated 6 sec postinjection. Brains were rapidly removed and frozen on dry ice. Twenty micron horizontal sections were cut on a cryostat, picked up onto cold glass cover slips and dried on a slide warmer at 60°C. XAR-5 x-ray film (Kodak, Rochester, NY) was exposed to the sections overnight and the film was then developed. Transilluminated autoradiograms were digitized and analyzed using an image analyzer (MCID image analysis system, Imaging Research, St. Catharine's, Canada).

Radiopharmaceutical Preparation

Technetium-99m-Cl(DMG)$_3$2MP was prepared using lyophilized kits as previously described (*14*). Technetium-99m-Cl(DMG)$_3$2MP was separated from other kit constituents using a Sep-Pak procedure (*27*) and the radiochemical purity (RCP) of the eluate was determined by HPLC (*14*).

Technetium-99m-ECD was prepared by mixing 0.8–1.2 mg (2.5–3.7 μmol) ethyl cysteinate dimer, 0.2 ml absolute ethanol, 0.3 ml USP saline, 0.5 ml TcO_4^-, 0.7 ml of 0.1 *M* $NaHCO_3$ and 20 μl of freshly prepared saturated stannous tartrate solution in a siliconized glass vial. The mixture was allowed to stand at

ambient temperature for 15 min and purified as described above for ^{99m}Tc-Cl(DMG)$_3$2MP, except that the resin was washed three times with 0.5 ml of 25% ethanol to remove hydrophilic components. Technetium-99m-ECD was removed with 0.5 ml USP absolute ethanol and collected in a siliconized glass vial. The RCP of the purified ^{99m}Tc-ECD was determined by HPLC on a Hamilton PRP-1 column (150 × 4.1 mm, 5 μ packing) eluted with 60% acetonitrile, 40% 0.1 *M* ammonium acetate buffer (pH 4.6) at a flow rate of 2.0 ml/min (R_T = 2.3 min).

Technetium-99m-HMPAO was prepared by mixing 2.8 mg (10.0 μmol) HMPAO·HCl, 0.5 ml of 0.1 *M* $NaHCO_3$, 0.5 ml USP saline, 0.5 ml $^{99m}TcO_4^-$ and 20 μl saturated stannous tartrate solution in a siliconized glass vial. The mixture was allowed to stand at ambient temperature for 5 min. Both the purification and HPLC analysis were done as described above for ^{99m}Tc-ECD (R_T = 2.1 min).

Iodine-123-IMP (Iofetamine HCL, 1 mCi/ml) was obtained from Medi+Physics (Arlington Heights, IL). At the time of use, the vial contained 2.58 mCi/3 ml and 0.45 mg IMP. Copper-67-PTSM was obtained from M. Welch at Washington University. Technetium-99m-DTPA was made from lyophilized kits (Squibb, Princeton, NJ) reconstituted in the normal manner. RCP was determined by paper chromatography as recommended in the package insert. Technetium-99m-pertechnetate in saline was obtained from a Squibb Minitec generator.

The RCP for all purified material was greater than 95% by HPLC. We found that RCP of purified ^{99m}Tc-HMPAO was stable at greater than 95% for several hours in absolute ethanol at 4°C, but decreased rapidly in physiological saline containing Tween-80 (0.05%), as expected based on the known chemical instability of this agent (*28*).

Microsphere and Injectate Preparation

Strontium-85-labeled polystyrene microspheres (Dupont-NEN, N. Billerica, MA) were used. Each vial of microspheres contained 500 μCi in a volume of 1.0 ml (0.9% saline with 0.01% Tween-80 added as a surfactant). The mean sphere size was 16.1 ± 0.1 μ and the number of microspheres per 1.0 ml vial was 15–18 × 10^6 depending on the batch. Prior to mixing with a test compound, the vial of microspheres was vortexed briefly, then sonicated in a water bath for 15–20 min. The preparation of the injection mixture depended on the desired injection volume and chemical stability of the compound. The single-pass cerebral extractions of ^{99m}Tc-Cl(DMG)$_3$2MP, ^{99m}Tc-HMPAO, ^{99m}Tc-ECD, ^{123}I-IMP, ^{67}Cu-PTSM, $^{99m}TcO_4^-$ and ^{99m}Tc-DTPA were determined by injecting a mixture of a single test agent (2.5 μCi) and radiolabeled microspheres (2.5 μCi) in 200 μl of physiological saline and Tween-80 (0.05%). Based on a 1.5% fractional distribution of cardiac output to rat brain (*29*), each brain received a minimum of 1,125–1,350 microspheres at normal CBF levels. We also examined the effect of intracardial injection volume (200 μl versus 50 μl) on the cerebral extraction of ^{99m}Tc-Cl(DMG)$_3$2MP and ^{99m}Tc-HMPAO. Owing to the instability of ^{99m}Tc-HMPAO in aqueous media, the ^{99m}Tc-HMPAO/^{85}Sr-labeled microsphere injection mixture was prepared and injected immediately.

Since the microspheres were suspended in Tween-80, we examined the effect of Tween-80 on extraction using ^{99m}Tc-Cl(DMG)$_3$2MP as a test substance. This was evaluated by determining the extraction of ^{99m}Tc-Cl(DMG)$_3$2MP relative to that of ^{123}I-IMP, which is highly extracted (*1*) in the presence and absence of Tween-80. Iodine-123-IMP was used as a "chemical microsphere" in lieu of ^{85}Sr-labeled microspheres to avoid macroaggregation of microspheres in the absence of Tween-80. Each sample to be injected contained 2.5 μCi of ^{99m}Tc-Cl(DMG)$_3$2MP and 2.5 μCi of ^{123}I-IMP in 200 μl of physiological saline with or without Tween-80 (0.05%). In the mixture without Tween-80, the sample was injected immediately after preparation to avoid chloro-to-hydroxy exchange at the axial position of ^{99m}Tc-Cl(DMG)$_3$2MP, which is known to occur with a half-time of 21 min at pH 7.4 and 37°C (*27*). This precaution was not necessary in the mixture containing Tween-80 because it stabilizes ^{99m}Tc-Cl(DMG)$_3$2MP in aqueous media.

Data Analysis

Following the method of Irwin and Preskorn (*23*), the single-pass cerebral extraction, E, was calculated using:

$$E = \frac{(CPM_{test}/CPM_{^{85}Sr})_{brain}}{(CPM_{test}/CPM_{^{85}Sr})_{blood}}. \qquad \text{Eq. 1}$$

Organ blood flows, OBF, (ml/g/min) were calculated using:

$$\text{OBF (ml/g/min)} = OBF_{^{85}Sr} = \frac{(1.15 \text{ ml min}^{-1})(CPM_{^{85}Sr})_{organ}}{(CPM_{^{85}Sr})_{blood}(\text{organ wt. g})}. \qquad \text{Eq. 2}$$

Data from the gamma counter were electronically captured and transferred to a spreadsheet. Blood gas values and organ weights were also entered into this spreadsheet. The data for E, OBF, P_aCO_2, P_aO_2, arterial blood pH and core temperature for each rat were then evaluated by a spreadsheet to screen for deviation from preset normal physiological range criteria. Data were rejected if any of the following events were observed:

1. P_aO_2 was below 50 mmHg. This criterion was designed to ensure that stimulation of CBF by hypercapnia was not associated with excessive hypoxia.
2. P_aCO_2 was between 37–43 mmHg and CBF was greater than 1.2 ml/g/min, a value arbitrarily selected as one substantially above the normal range for anesthetized rats. This criterion was designed to prevent inclusion of rats that were more lightly anesthetized than the others.
3. P_aCO_2 was above 60 and CBF was below 0.5 ml/g/min. Inclusion of rats with CBF that could not be stimulated by hypercapnia was prevented by this criterion, thereby excluding rats that may have been more deeply anesthetized than the others.
4. Renal or myocardial blood flow was greater than 10 ml/g/min. This criterion was designed to exclude cases of extreme organ blood flows.
5. Renal flow was below 0.05 ml/g/min. This criterion was designed to exclude rats that had severely reduced renal blood flow, which was potentially indicative of renal failure.
6. Temperature below 36°C or above 39°C.
7. Arterial pH below 7.1 or above 7.5.

Analysis of covariance was used to evaluate the relationship between measured values for E and CBF for ^{99m}Tc-Cl(DMG)$_3$2MP, ^{99m}Tc-ECD, ^{99m}Tc-HMPAO, ^{67}Cu-PTSM and ^{123}I-IMP. The model used was E = C + F + A + F × A, where E is the independent variable, A (agent) represents the dependent variable and F (flow) is the covariate. The F × A interac-

tion term was used to evaluate differences among the slopes of the regression lines for the agents tested. After grouping the agents according to similarity of slope, mean comparisons were made within parallel groups.

We substituted the measured values for E and $CBF_{^{85}Sr}$ in an equation derived from the Renkin-Crone model in order to determine the value of the PS. The model relates E, PS and flow (F) through a unit capillary according to:

$$E = 1 - e^{-PS/F}. \quad \text{Eq. 3}$$

Equation 3 can be applied to the entire brain capillary bed simply by substituting $CBF_{^{85}Sr}$ for F. S then refers to the surface area of the entire capillary component of the microcirculation and P represents permeability of the BBB to the extracted permeant. The average PS value for the microcirculation of whole brain can then be determined by solving the transformed and rearranged form of Equation 3:

$$PS = -\ln(1 - E)CBF_{^{85}Sr}. \quad \text{Eq. 4}$$

Once PS was determined in this manner, we used SYSTAT to determine the significance of linear and nonlinear terms in a polynomial model for the regression of PS on CBF. We were thus able to evaluate whether the relationship between PS and CBF could be described in terms of a simple linear model over the range of flows studied.

The ability of a test agent to measure true CBF was determined according to:

$$CBF_{test} = (E)CBF_{^{85}Sr}. \quad \text{Eq. 5}$$

Arbitrary uniformly incremental values for $CBF_{^{85}Sr}$ and corresponding values for E, determined from linear regression equations for the relationship between E and $CBF_{^{85}Sr}$, were substituted in Equation 5 to generate values for CBF_{test}. Then, CBF_{test} was plotted as a function of $CBF_{^{85}Sr}$ to compare the ability of the agents to measure CBF over a full range of clinically significant blood flows.

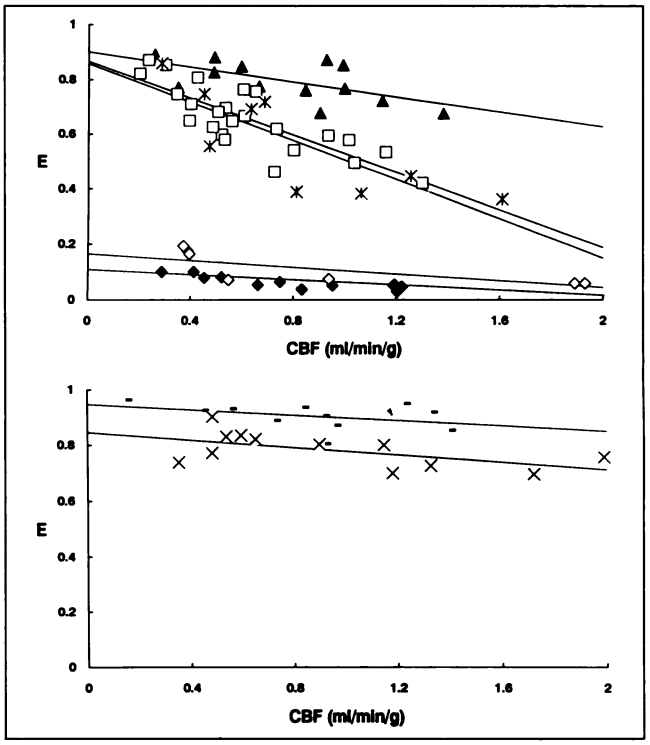

FIGURE 1. Scatter diagram showing single-pass cerebral extraction values obtained at each unique value of $CBF_{^{85}Sr}$ obtained in individual rats. The fit functions for the linear regressions of E on $CBF_{^{85}Sr}$ are shown for the groups of rats treated with the putative CBF imaging agents. (Top) Technetium-labeled compounds. ▲ = ^{99m}Tc-HMPAO (n = 13): y = −0.139 × +0.90, r = 0.62; □ = ^{99m}TcCl(DMG)$_3$2MP (n = 23): y = −0.34 × +0.87, r = 0.81; ✳ = ^{99m}Tc-ECD (n = 9): y = −0.355 × +0.859, r = 0.81; ◆ = $^{99m}TcO_4^-$ (n = 12): y = −0.046 × +0.11, r = 0.66; ◇ = ^{99m}Tc-DTPA (n = 6): y = −0.061 × +0.165, r = 0.74. (Bottom) Nontechnetium-labeled compounds. ■ = ^{123}I-IMP (n = 10): y = −0.052 × +0.947, r = 0.42; × = ^{67}Cu-PTSM (n = 12): y = −0.07 × +0.845, r = 0.59.

RESULTS

Extraction

We compared the performance of the various agents using analysis of covariance which requires the linear model, since we found that exponential regressions of E on CBF did not provide a better fit for the data over the range of flows studied (see Appendix). Figure 1 shows the relationship between extraction and CBF for the different compounds. Examination of this figure clearly demonstrates that the extraction of all the agents is substantially greater than that of ^{99m}Tc-DTPA and $^{99m}TcO_4^-$. Analysis of covariance by SYSTAT revealed no significant difference between ^{99m}Tc-Cl(DMG)$_3$2MP and ^{99m}Tc-ECD. The slopes of the regression equations of ^{99m}Tc-HMPAO, ^{67}Cu-PTSM and ^{123}I-IMP did not differ, but the intercept of the equation for ^{123}I-IMP differed from those of ^{67}Cu-PTSM and ^{99m}Tc-HMPAO ($p < 0.001$). Both the slopes and intercepts for the linear regressions of ^{99m}Tc-HMPAO, ^{67}Cu-PTSM and ^{123}I-IMP differed from those of ^{99m}Tc-ECD and ^{99m}Tc-Cl(DMG)$_3$2MP ($p < 0.02$). At a normal whole rat brain CBF level of 0.5 ml/g/min, the extractions of the agents were 0.92 (^{123}I-IMP); 0.83 (^{99m}Tc-HMPAO); 0.81 (^{67}Cu-PTSM); 0.70 (^{99m}Tc-Cl(DMG)$_3$2MP) and 0.68 (^{99m}Tc-ECD). It is evident from the R^2 values in Table A2 (Appendix) for the groups with the largest, ^{99m}Tc-Cl(DMG)$_3$2MP, and the smallest, ^{99m}Tc-ECD, sample size that differences in sample size did not influence our statistical analyses.

Effect of Tween-80 and Injection Volume on Extraction

The single-pass brain extraction of ^{99m}Tc-Cl(DMG)$_3$2MP relative to ^{123}I-IMP was 0.68 ± 0.05 (mean ± s.e.m., n = 6) in the presence of Tween-80 and 0.67 ± 0.04 (mean ± s.e.m., n = 6) without Tween-80 under conditions designed to produce normal blood flows, i.e., arterial P_aCO_2 set to 40 ± 3 mmHg. Analysis of covariance by SYSTAT revealed that intracardial injection volume had no effect on the extraction of ^{99m}Tc-Cl(DMG)$_3$2MP or ^{99m}Tc-HMPAO as shown in Figure 2.

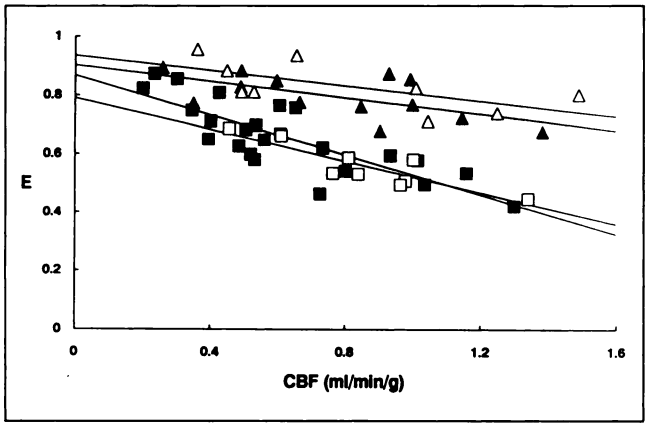

FIGURE 2. Comparison of single-pass extraction values obtained with different injection volumes of ^{99m}Tc-Cl(DMG)$_3$2MP and ^{99m}Tc-HMPAO. ▲ = ^{99m}Tc-HMPAO (200 μl) (n = 13): y = −0.139 × +0.90, r = 0.62; △ = ^{99m}Tc-HMPAO (50 μl) (n = 9): y = −0.131 × +0.936, r = 0.65; ■ = ^{99m}Tc-Cl(DMG)$_3$2MP (200 μl) (n = 23): y = −0.34 × +0.87, r = 0.81; □ = ^{99m}Tc-Cl(DMG)$_3$2MP (50 μl) (n = 9): y = −0.271 × +0.792, r = 0.88.

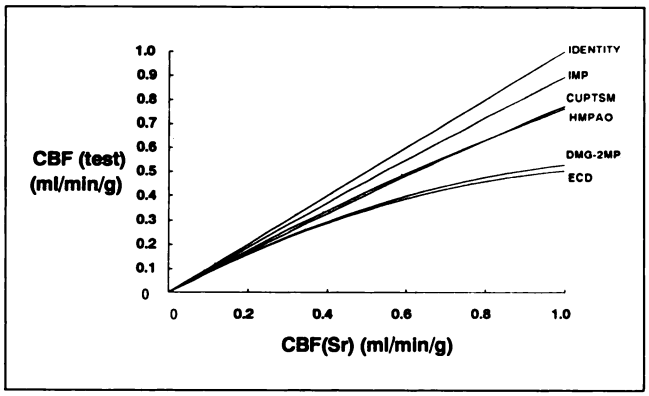

FIGURE 4. Estimated nonlinear fit functions for the regression of CBF_{test} on $CBF_{^{85}Sr}$ over the clinical range of CBF expected for human cortex. Values for CBF_{test} were obtained as described in the text.

PS Product

Nonlinear regression analysis revealed significant linear ($p < 0.03$) but nonsignificant quadratic ($p < 0.16$) terms for the polynomial regression of PS on CBF. The linear regressions for the relationship between PS and CBF are shown in Figure 3. For all agents, PS increased linearly with CBF. As expected from the extraction data, slopes of the regression equations for ^{99m}Tc-HMPAO, ^{67}Cu-PTSM and ^{123}I-IMP are greater than the slopes for the regression equations for ^{99m}Tc-Cl(DMG)$_3$2MP and ^{99m}Tc-ECD. Since all groups of rats were treated in the same manner, it is likely that the relationship between capillary surface area and CBF was similar in all groups. Consequently, any differences in the relationship between PS and CBF reflect differences in the apparent permeability of the BBB to the various compounds tested.

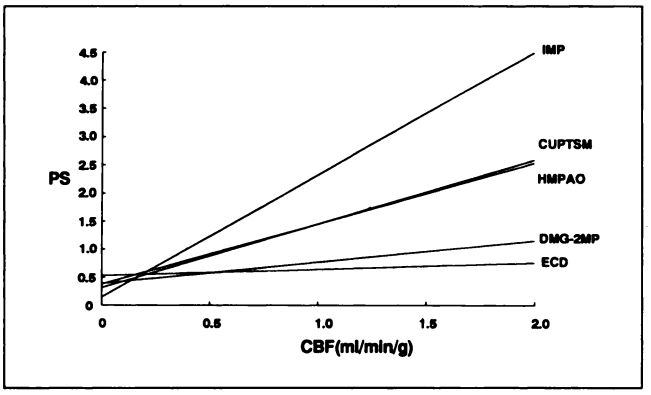

FIGURE 3. Composite of the fit functions for the linear regressions of PS on $CBF_{^{85}Sr}$. Values for PS were determined by substituting measured values for E and $CBF_{^{85}Sr}$ into PS = −ln(1 − E)$CBF_{^{85}Sr}$. ^{99m}Tc-HMPAO: y = 1.07 × +0.375, r = 0.80; ^{99m}Tc-Cl(DMG)$_3$2MP: y = 0.38 × +0.386, r = 0.66; ^{99m}Tc-ECD: y = 0.112 × +0.53, r = 0.29; ^{123}I-IMP: y = 2.166 × +0.146, r = 0.90; ^{67}Cu-PTSM: y = 1.131 × +0.314, r = 0.95.

Cerebral Blood Flow

Figure 4 shows the results obtained for the relationship between CBF_{test} and $CBF_{^{85}Sr}$ calculated from Equation 5 as described in the Methods section. The 1.0 ml/g/min cutoff value for $CBF_{^{85}Sr}$ was taken to illustrate the performance of a test agent over the clinical rCBF range for humans. For each of the compounds, the departure from the line of identity results from the decline in extraction as CBF increases. Consequently, as predicted by Equation 5, fidelity to true CBF is greater for ^{123}I-IMP, ^{99m}Tc-HMPAO and ^{67}Cu-PTSM than ^{99m}Tc-Cl(DMG)$_3$2MP and ^{99m}Tc-ECD.

Autoradiography

A brain autoradiogram, obtained from a rat decapitated 6 sec after left ventricular injection of ^{99m}Tc-Cl(DMG)$_3$2MP, is shown in Figure 5. Considerable microregional variation is present within the grey matter. The relationship of ^{99m}Tc-Cl(DMG)$_3$2MP distribution to true flow is depicted in Figure 4.

DISCUSSION

Analysis of covariance allowed us to demonstrate that ^{99m}Tc-HMPAO, ^{123}I-IMP and ^{67}Cu-PTSM have greater single-pass cerebral extractions than ^{99m}Tc-Cl(DMG)$_3$2MP and ^{99m}Tc-ECD across a full range of clinically significant CBFs. Generally, it is held that an ideal agent for imaging CBF would be highly extracted without decrement as CBF increases. It is apparent from Equation 3 that extraction will be higher for higher values of PS/CBF and lower for lower values of PS/CBF. Accordingly, for ^{99m}Tc-HMPAO, ^{123}I-IMP and ^{67}Cu-PTSM, we found that large positive slopes of the regression equations describing the relationship between PS and CBF (Fig. 3) are associated with high extraction values

FIGURE 5. Rat brain autoradiogram obtained 6 sec after the left ventricular injection of approximately 10 mCi of ^{99m}Tc-Cl(DMG)$_3$2MP. The autoradiogram, which is an image of relative CBF, clearly shows the CBF difference between grey and white matter. Considerable microregional heterogeneity of CBF within the cortex is also evident.

(Fig. 1). This analysis is also consistent with our observation of generally lower extraction values for ^{99m}Tc-Cl(DMG)$_3$2MP and ^{99m}Tc-ECD, which are characterized by smaller positive slopes of regression equations for the relationship between PS and CBF.

We did not replicate the previously observed volume dependence of the extraction of ^{99m}Tc-HMPAO (*8*). In that work, the extraction following an intracarotid injection was slightly reduced when the injection volume was lowered from 120 μl to 20 μl (*8*). This was attributed to a greater mixing-dependent sequestration of ^{99m}Tc-HMPAO by blood elements for the smaller injection volume. This raises the possibility that, whereas the intracarotid injection method of Andersen (*8*) resulted in mixing differences for the different injection volumes, our intracardial injection method produced an equal mixing of the two volumes we have used.

We found that PS increases as a linear function of CBF over the range of flows studied. While departures from linearity at the upper and lower levels of CBF may be expected on the basis of physiological considerations, these were not of sufficient magnitude over the range of flows we studied to be detectable as a quadratic component in a polynomial model for the regression of PS on CBF. An increase in PS with increasing CBF has been reported under a range of physiological conditions designed to determine extraction or BBB permeability (*8,23,26,30–33*). Indeed, Renkin found that PS increased dramatically in perfused muscle in a manner that was positively correlated with decreasing vascular resistance, i.e., increasing flow (*18*). Our data are in agreement with the preponderance of studies which demonstrate an increasing monotonic relationship between PS and CBF. On the other hand, an apparent lack of capillary recruitment in response to hypercapnia has been reported based on the failure of a fluorescent morphometric technique to detect an increase in the density of perfused capillaries, even though CBF increased in response to the increase in P_aCO_2 (*34*). This finding is supported by the demonstration, using a double-staining method for intravascular markers and the capillary wall, that morphologically identifiable capillaries are invariably perfused (*35*). It is worth mentioning, however, that the perfusion markers used by Gobel et al. (*34*) are plasma markers and provide no information concerning the circulation of erythrocytes. In fact, Villringer et al. (*36*) have found, using confocal scanning laser microscopy, that between 10% and 20% of brain capillaries are devoid of erythrocytes for periods up to 3 min while retaining plasma perfusion. During hypercapnia, the number of erythrocyte perfused capillaries as well as erythrocyte velocities increased. These data indicate that any material that is capable of being delivered to the brain parenchyma from an erythrocyte compartment may be exposed to a greater capillary surface area when flow increases. In a recent study of one of the BATOs, Rumsey et al. (*37*) showed that 72% of the ^{99m}Tc-teboroxime activity associated with erythrocytes during a 5-min preincubation is extracted during a single-pass through the isolated perfused rat heart. The extent to which other agents are also extractable from erythrocytes is unknown. However, it is quite likely that the highly diffusible alcohols used in studies cited above (*8,26,30, 32,33*) are readily extracted from erythrocytes. The possibility therefore arises that capillary recruitment for erythrocyte flow may contribute at least in part to reported observations of increased PS when CBF increases. In addition, capillary density and, therefore, PS product may also vary microregionally within the cortex (*26*). The considerable heterogeneity of relative CBF evident in the autoradiogram shown in Figure 5 is consistent with this conjecture. Thus, a limitation of the present experiments is that they determined values that are averages for whole brain. Nevertheless, if it is assumed that the relationship achieved between whole brain capillary surface area and CBF was the same for all the groups in the present studies, the various slopes depicted in Figure 4 can be interpreted as measures of the average relative permeability of the BBB to the different compounds studied.

The data shown in Figure 4 represent the maximum potential fidelity of each agent to true CBF over a full range of flows. These data show that, under optimal single-pass conditions, changes in true (microsphere) CBF are detected reasonably well by all the agents in the ischemic to normal range of flows, but that ^{123}I-IMP, ^{67}Cu-PTSM and ^{99m}Tc-HMPAO show greater fidelity to true CBF than ^{99m}Tc-Cl(DMG)$_3$2MP and ^{99m}Tc-ECD. The underestimation of true flow by all the agents increased and the difference among the agents became more extreme at higher flows. The significance of these findings for clinical imaging studies must take account of the affect of time on brain retention of the agents and the

TABLE A1
Linear Regression Equations for the Regression of $-\ln(1 - E)$ on 1/CBF and the Regression of PS on CBF for Each of the Putative CBF Imaging Agents Tested

Compound	$-\ln(1 - E) = C_1/CBF + C_2$	$PS = C_1 + C_2$ (CBF)
^{99m}Tc-Cl(DMG)$_3$2MP	$-\ln(1-E) = 0.32/CBF + 0.50$	PS = 0.32 + 0.50 (CBF)
^{99m}Tc-ECD	$-\ln(1-E) = 0.52/CBF + 0.13$	PS = 0.52 + 0.13 (CBF)
^{99m}Tc-HMPAO	$-\ln(1-E) = 0.23/CBF + 1.28$	PS = 0.23 + 1.28 (CBF)
^{67}Cu-PTSM	$-\ln(1-E) = 0.19/CBF + 1.29$	PS = 0.19 + 1.29 (CBF)
^{123}I-IMP	$-\ln(1-E) = 0.18/CBF + 2.12$	PS = 0.18 + 2.12 (CBF)

radioactivity in brain relative to extracerebral tissue background.

APPENDIX

Linearity Versus Nonlinearity of the Relationship Between E and CBF

We have shown that the relationship between PS and CBF is linear over the range of flows studied. Here we further characterize the nature of this relationship using another approach; in particular, whether PS is constant with respect to CBF. We then derive an algebraic expression for PS in terms of CBF that can be substituted into the numerator of the Renkin-Crone equation to render the expression a function of one variable. This allows us to use the Renkin-Crone equation as an exponential regression model as described below. The rearranged form of Equation 4:

$$-\ln(1 - E) = PS(1/CBF) \qquad \text{Eq. 6}$$

is in the form of a linear equation if PS is assumed to be constant. In this case, PS is the slope of the linear equation derived from the linear regression of $-\ln(1 - E)$ on 1/CBF. To evaluate the assumption that PS does not vary with respect to CBF, we determined the linear regression of $-\ln(1 - E)$ on 1/CBF for each of the compounds tested, which yielded regression equations of the general form:

$$-\ln(1 - E) = C_1/CBF + C_2, \qquad \text{Eq. 7}$$

where C_1 and C_2 are constants. As seen in Table A1, in every case C_2 is substantial with respect to C_1. Comparing Equation 7 to Equation 6, it is evident that:

$$PS/CBF = C_1/CBF + C_2 \qquad \text{Eq. 8}$$

and therefore

$$PS = C_1 + C_2(CBF). \qquad \text{Eq. 9}$$

This result shows that, owing to the presence of a substantial intercept term (C_2) in Equation 7 which appears as the cofactor of CBF in Equation 9, PS is not constant and must be treated as a linear function of CBF over the range of flows studied. The equations for PS are shown for each agent in Table A2.

The linear expressions for PS shown in Table A2 then were substituted in the numerator of the exponent of Equation 3 to yield an equation of the form:

$$E = 1 - e^{-\{[C_1 + C_2(CBF)]/CBF\}}. \qquad \text{Eq. 10}$$

Equation 10 then was applied as an exponential model for the regression of E on CBF using SYSTAT. Linear regressions for the relationship between E and $CBF^{as}{}_{Sr}$ then were determined by analysis of covariance using SYSTAT. Next, to evaluate the relative goodness of fit provided by linear and exponential regressions of E on CBF, R^2 values obtained from the respective analyses were compared as shown in Table A2.

The comparison of R^2 values for the linear and exponential regressions of E on CBF shows that the two models do not differ with respect to goodness of fit. Since the R^2 values are similar, we chose the linear model on the basis of using the simplest model to fit the data. Therefore, we were able to use analysis of covariance, which is based upon the linear model, to compare the relationship between E and CBF among the various agents tested, as shown in Methods and Results.

TABLE A2
Comparison of R^2 Values Obtained for Linear and Exponential Regressions of E on CBF for Each of the Putative CBF Imaging Agents Tested

Compound	Linear R^2	Exponential R^2
^{99m}Tc-Cl(DMG)$_3$2MP	0.67	0.68
^{99m}Tc-ECD	0.67	0.73
^{99m}Tc-HMPAO	0.38	0.30
^{67}Cu-PTSM	0.35	0.23
^{123}I-IMP	0.18	0.25

ACKNOWLEDGMENTS

The authors thank L. Belnavis, C. Hood and M. Homak for their technical assistance; Dr. T. Graves for his statistical advice; Drs. W.R. Rumsey and D.P. Nowotnik for their helpful advice and comments on the manuscript; Dr. J. Fenstermacher for his helpful comments concerning the important distinction between erythrocyte and plasma perfusion; and Dr. M. Welch for supplying ^{67}Cu-PTSM.

REFERENCES

1. Winchell HS, Horst WD, Braun L, Oldendorf WH, Hattner R, Parker H. N-isopropyl-[^{123}I] p-iodoamphetamine: single-pass brain uptake and washout; binding to brain synaptosomes; and localization in dog and monkey brain. *J Nucl Med* 1980;21:947–952.
2. Ell PJ, Cullum I, Donaghy M, Lui D, Jarritt PH, Harrison MJG. Cerebral blood flow studies with ^{123}I-labeled amines. *Lancet* 1983;11:1348–1352.
3. Podreka I, Baumgartener C, Suess E, et al. Quantification of regional cerebral blood flow with IMP-SPECT. *Stroke* 1989;20:183–191.
4. Green MA. A potential copper radiopharmaceutical for imaging the heart and brain: copper-labeled pyruvaldehyde *bis*(N4-methylthiosemicarbazone). *Nucl Med Biol Int J Radiat Appl Instrum Part B* 1989;14:59–61.

5. Green MA, Klippenstein DL, Tennison JR. Copper(II) *bis*(thiosemicarbazone) complexes as potential tracers for evaluation of cerebral and myocardial blood flow. *J Nucl Med* 1988;29:1549–1557.
6. Volkert W, McKenzie EH, Hoffman TJ, Troutner DE, Holmes RA. The behavior of neutral amine oxime chelates labeled with technetium at tracer levels. *J Nucl Med Biol* 1984;11:243–246.
7. Nowotnik DP, Canning LR, Cumming SA, et al. Development of a ^{99m}Tc-labeled radiopharmaceutical for cerebral blood flow imaging. *Nucl Med Commun* 1985;6:499–506.
8. Andersen AR, Friberg H, Knudsen KBM, et al. Extraction of [^{99m}Tc]-d,I,HM-PAO. *J Cereb Blood Flow Metab* 1988;8:S44–S51.
9. Vallabhajosula S, Zimmermann RE, Picard M, et al. Technetium-99m ECD: a new brain imaging agent: in vivo kinetics and biodistribution studies in normal human subjects. *J Nucl Med* 1989;30:599–604.
10. Walovitch RC, Hill TC, Garrity ST, et al. Characterization of technetium-99m-L,L-ECD for brain perfusion imaging: part 1: pharmacology of technetium-99m ECD in nonhuman primates. *J Nucl Med* 1989;30:1892–1901.
11. Leveille J, Demonceau G, De Roo M, et al. Characterization of technetium-99m-L,L-ECD for brain perfusion imaging: part 2: biodistribution and brain imaging in humans. *J Nucl Med* 1989;30:1902–1910.
12. Treher EN, Francesconi LC, Gougatas JZ, Malley MF, Nunn AD. Monocapped *tris*(dioxime) complexes of technetium(III): synthesis and structural characterization of $TcX(dioxime)_3B$-R(X = Cl, Br; dioxime = dimethylglyoxime, cyclohexanedione dioxime; R = CH_3, C_4H_9). *Inorg Chem* 1989;28:3411–3416.
13. Linder KE, Malley MF, Gougoutas JZ, Unger SE, Nunn AD. Neutral seven-coordinate dioxime complexes of technetium (III): synthesis and characterization. *Inorg Chem* 1990;29:2428–2434.
14. Narra RK, Nunn AD, Kuczynski BL, et al. A neutral lipophilic ^{99m}Tc complex for regional cerebral blood flow imaging. *J Nucl Med* 1990;31: 1370–1377.
15. Sapirstein LA. Regional blood flow by fractional distribution of indicators. *Am J Physiol* 1958;193:161–168.
16. Devous MD, Payne JK, Lowe JL. Extraction, retention and kinetics of ^{99m}Tc-ECD and HMPAO following intracarotid injection in cynomolgus monkeys. *J Nucl Med* 1989;30(suppl 5):742.
17. Lucignani G, Rossetti C, Otsuki H, Chelliah M, Blasberg R, Sokoloff L. Evaluation of SQ 32097: a ^{99m}Tc labeled tracer for measuring CBF. *J Cereb Blood Flow Metab* 1989;9(suppl 1):S205.
18. Renkin E. Transport of potassium-42 from blood to tissue in isolated mammalian skeletal muscles. *Am J Physiol* 1959;197:1205–1210.
19. Crone C. The permeability of capillaries in various organs determined by use of the indicator diffusion method. *Acta Physiol Scand* 1963;58:292–305.
20. Furlow THW, Bass NH. Cerebral hemodynamics in the rat assessed by a nondiffusible indicator-dilution technique. *Brain Res* 1976;110:366–370.
21. Hardebo JE, Nilsson B. Estimation of cerebral extraction of circulating compounds by the brain uptake index method: influence of circulation time, volume injection and cerebral blood flow. *Acta Physiol Scand* 1979;107:153–159.
22. Saris SC, Wright DC, Oldfield EH, Blassberg RG. Intravascular streaming and variable delivery to brain following carotid artery infusions in the Sprague-Dawley rat. *J Cereb Blood Flow Metab* 1988;8:116–120.
23. Irwin GH, Preskorn SH. A dual label radiotracer technique for the simultaneous measurement of cerebral blood flow and the single-transit cerebral extraction of diffusion-limited compounds in the rat. *Brain Res* 1982; 249:23–30.
24. Eichling JO, Raichle ME, Grubb RL, Ter-Pogossian MM. Evidence of the limitations of water as a freely diffusible tracer in the brain of the rhesus monkey. *Circ Res* 1974;35:358–364.
25. Raichle ME, Eisling JO, Straatman MG, Welch MJ, Larson KB, Ter-Pogossian MM. Blood-brain barrier permeability of ^{11}C-labeled alcohols and ^{15}O-labeled water. *Am J Physiol* 1976;230:543–552.
26. Herscovitch P, Raichle ME, Kilbourn MR, Welch MJ. Positron emission tomographic measurement of cerebral blood flow and permeability-surface area product of water using [^{15}O]water and [^{11}C]butanol. *J Cereb Blood Flow Metab* 1987;7:527–542.
27. Jurisson S, Hirth W, Linder KE, et al. Chloro/hydroxy substitution on technetium BATO ($TcCl(dioxime)_3BR$) complexes. *Nucl Med Biol* 1991; 18:735–744.
28. Neirinckx RD, Canning LR, Piper IM, et al. Technetium-99m d,I,-HM-PAO: a new radiopharmaceutical for SPECT imaging of regional cerebral perfusion. *J Nucl Med* 1987;28:191–202.
29. Nishiyama K, Nishiyama A, Frolich ED. Regional blood flow in normotensive and spontaneously hypertensive rats. *Am J Physiol* 1976;230:691–698.
30. Bowlig TG, Hertz MM, Paulson OB, Spotoft H, Rafaelsen OJ. The permeability of the blood-brain barrier during electrically-induced seizures in man. *Eur J Clin Invest* 1977;7:87–93.
31. Hertz MM, Paulson OB. Transfer across the human blood-brain barrier: evidence for capillary recruitment and for a paradox glucose permeability increase in hypocapnia. *Microvasc Res* 1982;24:364–376.
32. Pardridge WM, Frier G. Blood-brain transport of butanol and water relative to N-isopropyl-p-iodoamphetamine as the internal reference. *J Cereb Blood Flow Metab* 1985;5:275–281.
33. Phelps ME, Huang SC, Hoffman EJ, Selin C, Kuhl DE. Cerebral extraction of ^{13}N-ammonia: its dependence on cerebral blood flow and capillary permeability-surface area product. *Stroke* 1981;2:607–619.
34. Gobel U, Burkhard K, Schrock H, Kuschinsky W. Lack of capillary recruitment in the brains of awake rats during hypercapnia. *J Cereb Blood Flow Metab* 1989;9:491–499.
35. Kuschinsky W, Theilen H. Evidence for a continuous perfusion of all capillaries in the brain of the conscious rat. *J Cereb Blood Flow Metab* 1991;11(suppl 2):80.
36. Villringer A, Dirnagel U, Gebhardt R, Einhaupel KM. An in vivo approach to assess the capillary recruitment hypothesis in the brain microcirculation using confocal laser scanning microscopy. *J Cereb Blood Flow Metab* 1991;11(suppl 2):441.
37. Rumsey WL, Rosenspire K, Nunn AD. Myocardial extraction of teboroxime: effects of teboroxime interaction with blood. *J Nucl Med* 1992;33: 94–101.